

Analysis of myocardial motion using generalized spline models and tagged magnetic resonance images

Fang Chen^{* a}, Stephen E. Rose^a, Stephen J. Wilson^a, Martin Veidt^b, Cameron J. Bennett^c
and David M. Doddrell^a

^a Centre for Magnetic Resonance, University of Queensland, Brisbane Qld 4072, Australia.

^b Department of Mechanical Engineering, University of Queensland, Qld 4072, Australia.

^c Department of Internal Medicine, Royal Brisbane Hospital, Brisbane Qld 4029, Australia.

ABSTRACT

Heart wall motion abnormalities are the very sensitive indicators of common heart diseases, such as myocardial infarction and ischemia. Regional strain analysis is especially important in diagnosing local abnormalities and mechanical changes in the myocardium. In this work, we present a complete method for the analysis of cardiac motion and the evaluation of regional strain in the left ventricular wall. The method is based on the generalized spline models and tagged magnetic resonance images (MRI) of the left ventricle. The whole method combines dynamical tracking of tag deformation, simulating cardiac movement and accurately computing the regional strain distribution. More specifically, the analysis of cardiac motion is performed in three stages. Firstly, material points within the myocardium are tracked over time using a semi-automated snake-based tag tracking algorithm developed for this purpose. This procedure is repeated in three orthogonal axes so as to generate a set of one-dimensional sample measurements of the displacement field. The 3D-displacement field is then reconstructed from this sample set by using a generalized vector spline model. The spline reconstruction of the displacement field is explicitly expressed as a linear combination of a spline kernel function associated with each sample point and a polynomial term. Finally, the strain tensor (linear or nonlinear) with three direct components and three shear components is calculated by applying a differential operator directly to the displacement function. The proposed method is computationally effective and easy to perform on tagged MR images. The preliminary study has shown potential advantages of using this method for the analysis of myocardial motion and the quantification of regional strain.

Key words: Tagged magnetic resonance images, snakes tracking, cardiac diastole, myocardial motion, generalized spline models, displacement field reconstruction.

1. INTRODUCTION

The study of the mechanical properties of the human heart is of paramount importance in the diagnosis and treatment of most forms of heart disease. Global measures of pump efficiency using echocardiography often hide regional muscle abnormalities. Radionuclide studies have given some spatial information but lacked in spatial resolution^{1,2}. Tagged magnetic resonance imaging can generate images from which three dimensional motion over time of small regions of heart wall can be obtained. In recent years, this technique has been successfully used in the non-invasive assessment of myocardial motion during the entire cardiac cycle^{3,4,5}.

In tagging experiments, a set of parallel material tag planes throughout the myocardium is created orthogonal to the imaging plane of interest. The signal intensity of the tagged tissue decreases sharply, therefore tag lines appear as dark stripes at the intersection of the imaging plane and tagging planes. The tag lines deform with the myocardial tissue during the cardiac cycle. The deformation of the tags can be tracked point by point from their initial positions and the tracked distances provide directional measurements of the true three-dimensional displacement field of motion. By selecting several sets of tag planes in different orientations, different directional measurements can be tracked within the myocardium.

* Correspondence: Email: fiona@cmr.uq.edu.au; WWW:<http://www.cmr.uq.edu.au/~fiona>; Telephone: 61 7 3365 9065; Fax: 61 7 3365 3833

The reconstruction of myocardial motion from tagged MR images has generated much research interest in the field of non-rigid motion analysis and medical image reconstruction. In the literature, energy-minimizing based models are used most often for 3D myocardial surface fitting and motion analysis. These include, for example, a thin-plate spline model⁶, a bending and stretching spline models^{7,8}, energy-minimizing finite element models^{9,10}, snake based motion tracking approaches^{11,12}, as well as the spline with tension based dynamic deformable models^{13,14}. In these existing spline models or spline-based models, either a second order or a combination of the first and second order smoothness constraint in the objective function was used. Recently, a higher order spline model¹⁵ has been developed for motion field reconstruction. The model is generalized from the thin-plate spline and is defined by minimizing energy functional that contains multiple orders of the smoothness. This model is more suitable for solving complicated problems where the smoothness properties of the approximated functions are unknown or they may vary with regions.

In this paper, we present a numerical approach for the analysis of myocardial motion and the quantification of regional wall strain using tagged MR images and generalized vector splines. To capture the directional movement of myocardial tissue, we firstly develop a snake based tag tracking algorithm working on tagged MR images to track tag points (i.e. underlying material points) motion¹⁶. A number of selected tag points are tracked at different time instants during cardiac diastole and the corresponding directional movements of these sample points are calculated for the full displacement field reconstruction. It should be noted that the measured deformation of the sample points does not provide the complete displacement measurements but only the directional measurements, i.e. the projection of the displacement vector onto a given direction. The 3D displacement field is then recovered by fitting the sample projections with the generalized vector splines¹⁵. Regional strain tensors representing the deformation of cardiac tissue are determined based on the reconstructed displacement field.

The paper is structured as follows: The following section describes the tag tracking algorithm and implementation specification of performing the algorithm on tagged MR images. The displacement field reconstruction and strain analysis is studied in section 3. Finally, experimental results are presented and discussed.

2. TAG DEFORMATION TRACKING

2.1. Active Contour Algorithm

Tagged MR images are acquired by the application of a set of parallel tag planes orientated orthogonal to the imaging plane. The intersection of the image plane and tag plane appears as a dark line in the image, which is denoted as a tag line. These tag lines then deform with the motion of the heart, as illustrated in Figure 1. Deformation of the tag lines thus reflects the real motion of the myocardial tissue during the cardiac cycle. Therefore, the first stage of measuring the displacement field is to accurately monitor the deformation of the tag points.

In our work, the tag deformation is tracked based on a general active contour or *snakes* model¹⁶. In this model, a snake is defined as a continuity-controlled spline acted upon by an internal energy E_{internal} , an image energy E_{image} and an external energy E_{external} . A deformable contour is derived by minimizing a total energy functional E_{snake} . Suppose a snake is parametrically represented by a vector, $\mathbf{V}(s) = (x(s), y(s))$ ($0 < s < 1$), the total snake energy functional is:

$$E_{\text{snake}}(\mathbf{v}(s)) = \int_0^1 E_{\text{internal}}(\mathbf{v}(s))ds + \int_0^1 E_{\text{image}}(\mathbf{v}(s))ds + \int_0^1 E_{\text{external}}(\mathbf{v}(s))ds. \quad (1)$$

The internal energy controls the continuity and the smoothness of the contours and is composed of a first-order derivative (stretching energy) and a second-order derivative (bending energy) of the contour:

$$E_{\text{internal}}(\mathbf{v}(s)) = \frac{1}{2} \left[\alpha \left\| \frac{d\mathbf{v}(s)}{ds} \right\|^2 + \beta \left\| \frac{d^2\mathbf{v}(s)}{ds^2} \right\|^2 \right], \quad (2)$$

where α and β are weights associated with continuity and curvature and can be adjusted to control the continuity and smoothness of the contour.

The image energy is designed to attract the snake to image features. In our tag-tracking algorithm, the image energy is composed of image intensity $G(x,y)$ and the gradient of the image intensity $\nabla G(x,y)$. The image intensity attracts the snakes to move towards darker pixels and the gradient of the image intensity attracts the snakes to strong edges in the image, since tag lines in a tagged MR image appear dark and are recognized as edges.

Difficulties may occur when some of the tag deformations become quite large, that is, some tags move far from their previous positions so that the corresponding tag snakes have difficulties in finding the correct image feature. In this case, user interaction is very effective to locally guide the snakes to the desired positions. We add an external force (driven by mouse control) which enables the snakes to be pulled along the correct directions. This external interaction is very flexible and easy to perform.

Minimizing the snake energy (1) is associated with Euler-Lagrange equation:

$$\frac{\delta E_{\text{snake}}}{\delta \mathbf{v}} = \mathbf{0},$$

which can be discretized by finite differences to obtain an iterative solution^{11,17}:

$$\mathbf{v}^{k+1} = (A + h_t I)^{-1} [\mathbf{v}^k + h_t g(\mathbf{v}^k)], \quad k = 0, 1, \dots \quad (3)$$

where \mathbf{v}^{k+1} and \mathbf{v}^k are the $(k+1)$ -th and k -th iterations respectively. I denotes the identity matrix, h_t is a time step constant, and $g = \delta E_{\text{image}} / \delta \mathbf{v}$. The coefficient matrix $(A + h_t I)$ is a pentadiagonal banded symmetric matrix. Therefore, the iterative equation (3) can be solved using a common LU decomposition.

2.2. Implementation Details

To perform the tag tracking algorithm on tagged MR image includes three stages: manually setting contours and initial tag lines; automatically tracking tags followed by calculating the distance due to deformation. At the first stage, the epicardial and endocardial contours are drawn by a physician (CB). In fact, our snake algorithm can also work for tracking these two contours. However more user intervention is required for recognition of the boundary of the left and right ventricles in epicardial contour detection. In addition, exclusion of papillary muscle from the endocardial contour is also an added challenge for a fully automatic program. Most published contour/tag detection algorithms included some manual corrections¹⁸ or manually drawn contours¹² when tracking tagged MR images.

A graphical user interface has been developed on a Silicon Graphics workstation that provides a means of drawing contours on the images and to manually correct local errors. The manual correction, performed by mouse control, adds an external point force that attracts the nearby points (moving them towards the point of the applied force). The tag-tracking algorithm starts at the first time frame. Once the epicardial and endocardial contours are drawn, a training set of parallel initial lines are set to overlay the tag lines in the image. The algorithm then automatically duplicates these drawings to the next time frame. The user has two choices for processing contours: local modification by adding in mouse force or redrawing if the shape of the contours was dramatically changed. The tag snakes (each tag line is an open rather than closed loop snake) then automatically search for their optimal position in the current image. The user can control the number of iterations of snakes and can also undertake manual interaction during searching. When the user is satisfied with the tag tracking, tag lines outside of the myocardial tissue are removed from the image, see the third column in Figure 1. The whole processing – initial setting, searching and cutting - is then repeated in the following time frames.

To calculate the displacement components of individual points on tag lines for each time frame, the tags within the myocardium are sampled as discrete points separated by 1 pixel (about 1.56mm). These points are then projected to the corresponding initial tag lines and the distances between the sample points and their projections are calculated and saved for displacement reconstruction.

It is important to address the problems associated with 3D heart motion. The short axis images can only capture in-plane motion in two directions. If we choose the 45° tag orientation[†] as the x direction and the 135° tag orientation as the y direction, the sample distances calculated from the short axis slices represent the projections of the 3D displacement vector in only the x or y directions. Similarly, the long axis images capture the one dimensional through-plane motion. Using the LV central axis as the z direction, the sample distances calculated from the long axis slices are the projections of the displacement vectors in the z direction. Thus, the data samples obtained consist of three orthogonal directional projection measurements of the total 3D displacement vectors at discrete points on individual tag lines.

3. MOTION ANALYSIS

3.1. Displacement Field Reconstruction

Once the directional projections have been tracked in all possible directions (containing at least three orthogonal directions), a generalized vector spline model¹⁵ is used to reconstruct the displacement vector in 3D from these sample projections. Let $r_i (i = 1, \dots, N)$ be a set of 3D points, d_i be the projection measurement of displacement vector at r_i on a given direction \mathbf{n}_i . A vector spline reconstruction \mathbf{f} of the displacement field is defined to minimize the following smoothness energy functional:

$$\frac{1}{N} \sum_{i=1}^N [\mathbf{f}(r_i) \cdot \mathbf{n}_i - d_i]^2 + \lambda \int_{R^3} \sum_{m \leq \xi \leq m+l} \tau_{\xi} |D^{\xi} \mathbf{f}|^2 dr \quad (4)$$

where m and l are integers, λ and τ_{ξ} are model parameters. The projection operator is defined as an inner product of the displacement vector and the given direction. Using the standard vector derivative and multi-index notations, it follows that:

$$\frac{d\mathbf{f}}{dx} = \frac{df_1}{dx} \mathbf{e}_1 + \frac{df_2}{dx} \mathbf{e}_2 + \frac{df_3}{dx} \mathbf{e}_3 \quad \text{and} \quad D^{\xi} = \sum_{|\xi|=\xi_1+\xi_2+\xi_3} \frac{\partial^{|\xi|}}{\partial x^{\xi_1} \partial y^{\xi_2} \partial z^{\xi_3}},$$

where $(\mathbf{e}_1, \mathbf{e}_2, \mathbf{e}_3)$ is a 3D orthonormal basis.

The generalized vector spline model (4) provides a multiple control of the smoothness of the spline approximation. It allows us to fit data to a function with arbitrary order of smoothness. Along with a set of adjustable weights τ_{ξ} , we can easily control the relative magnitude of each order of smoothness in the whole smoothness functional. The overall goodness of fit and smoothness of spline reconstruction is controlled by another parameter λ , which can be forced to 0 to obtain a pure interpolatory spline or to ∞ to obtain a least square linear regression. As the data obtained from the tag-tracking algorithm contain noise, a smoothing spline rather than an interpolatory spline is employed to reconstruct the displacement field of cardiac motion.

Solving the minimization problem (4), a vector spline reconstruction can be explicitly expressed as a combination of the spline kernel function with a polynomial term:

$$\mathbf{f}(r) = \sum_{i=1}^N c_i K(|r - r_i|) \cdot \mathbf{n}_i + \mathbf{p}(r). \quad (5)$$

Since the smoothness functional (4) is invariant to translation and rotation, the spline models used here - unlike some of coordinate dependent approximation methods such as¹⁹ - are independent on the selection of a coordinate system. The following experiments are based on a 3D Cartesian coordinate system with the z direction orthogonal to the short axis

[†] As commonly defined, the angles we used here refer to a horizontal baseline and are rotated in anti-clockwise direction.

image plane pointing from apex to base and the x, y axes corresponding to the 45° and 135° tag directions on the short axis images.

The sample data are converted to the new coordinate system and are used in equation (5) to solve for the kernel coefficients c_i and the polynomial coefficients. For points derived from the short axis images and originally located at tags parallel to the y axis (135°) or x axis (45°), the direction vector is $\mathbf{n}(r) = \{1,0,0\}$ or $\mathbf{n}(r) = \{0,1,0\}$. For points derived from the long axis images, the direction vector is $\mathbf{n}(r) = \{0,0,1\}$.

3.2. Strain Determination

The myocardial strain is an important quantity that gives a complete description of the local shape change at each point within the myocardium. According to continuum mechanics theory²⁰, the strain tensor at a spatial point is defined as a symmetric matrix of six independent components with three direct strains and three shear strains. The direct strains describe the stretching or shorting along three orthogonal coordinate directions, while the shear strains describe the angular changes in each of the three coordinate planes.

As discussed above, the displacement field of the motion reconstructed by spline fitting defines a 3D map from spatial points (at the deformed time frame) to material points (at the first time frame which is considered to define the undeformed or reference configuration). This refers to a *backward* reconstruction. To analyze material deformation during heart motion, a *forward* reconstruction step is critical to determine the Lagrangian strain components at material points. In our study, an inverse operator is applied to predescribed spline method to obtain a forward mapping function. This forward function establishes a spatial correspondence from the material points to the spatial points. Similar to the backward reconstruction, the forward reconstruction results in an explicit expression that can be easily differentiated to calculate the components of the strain tensor at any location within the myocardium. Therefore, the proposed model provides a computational effective approach to evaluate both linear and nonlinear strain.

The nonlinear Lagrangian strain tensor is defined as:

$$\varepsilon_{ij} = \frac{1}{2} \left[\frac{\partial f_i}{\partial x_j} + \frac{\partial f_j}{\partial x_i} + \sum_{k=1}^3 \frac{\partial^2 f_k}{\partial x_i \partial x_j} \right], \quad i, j = 1, 2, 3$$

from which, the direct strain ε_{ii} and shear strain $\varepsilon_{ij} (i \neq j)$ can be calculated from a given displacement function $\mathbf{f} = (f_1, f_2, f_3)$. To compare regional strain, the LV wall is divided into small elements, each with eight nodes, and the local strain within each element is estimated by averaging the nodal values. The nodes are uniformly selected on the epicardial and endocardial surfaces of the LV wall. Analysis of these local strains over time enables to locate the regions of interest.

4. EXPERIMENTS AND RESULTS

4.1. Data Acquisition

Cardiac imaging experiments were performed on a Bruker Medspec S200 imaging system, interfaced to an Oxford Magnet Technology 2T whole-body magnet. Images were acquired in CINE mode using a spoiled GRASS sequence with ECG triggering and breath hold to reduce respiratory motion artifacts. The raw data for CINE MRI was sampled using a segmented k space acquisition. The imaging parameters were: field of view - 40cm, matrix size - 256x128 (zero filled to 256x256), TR - 7.5ms, TE - 2.4ms, flip angle - 20° slice thickness - 10mm. The number of phase encoded views per heartbeat was 8. Images were acquired over 16 consecutive heartbeats. Tagging was achieved by selectively inverting the magnetization in a plane perpendicular to the imaging plane. In this way, 8 parallel 1.5mm thick tags were generated with an inter-tag spacing of 10mm. For the short axis slices, the tag lines were placed at an 45° and an 135° angles in the imaging plane. In addition, the polarity of the tag gradients were swapped between the first eight and second eight heartbeats within a given breath hold scan. By utilizing an additive minimization step, high-resolution grid sampling was achieved.

Six contiguous double oblique short axis tagged images of the left ventricle were acquired from apex to base in CINE mode. Tagging was set at end systole in the cardiac cycle to allow for the monitoring of diastolic motion. Six corresponding orthogonal long axis slices with parallel tags sharing a common axis with the short axis slices were similarly acquired. The long axis slices were separated by 30° arc in a radial fashion. Six CINE frames with a temporal resolution of 40ms were used in the analysis.

4.2. Results

The tag-tracking algorithm described above was employed to calculate the distance of tag points from their initial position to their deformed location. In our experiments, the first time frame in each sequence is used as an initial reference frame. The results of tag deformation tracking are illustrated in Figure 1. The first and second rows show a short axis slice at mid-wall with 45° and 135° tags, and the last row shows a long axis slice with a set of parallel tags. Images shown in the left column are the first frames of the time series and correspond to tagging at end systole. The images in the second column are the final time frames and were acquired approximately 300ms into diastole. The deformation of tags at the final time frames was tracked and shown in the third column with outlined epicardial and endocardial contours. In the last column, the motion of the tag point was depicted by vectors from the deformed points to their initial reference positions and shown in a selected region of interest. For demonstrating purpose, only a subset of the tag points are shown.

In our experiments, five sets of sample data are derived by measuring the tag deformation of the corresponding five time frames from the first time frame. Each sample set includes a number of points that are located on the deformed tags, as well as the corresponding projection measurements to a given direction. The 3D projection measurements are illustrated in Figure 2 using only a small sample set. Projections of the displacement vectors along the x and y directions are shown in (a) from a short axis view and the projections along the z direction are shown in (b) from a long axis view.

Following the two-way reconstruction discussed above, a 3D map from material point to spatial point was established, from which the Lagrangian strain was calculated at the selected material points within the myocardium. Repeating this procedure to the following time sequence, the change of strain over time can be observed. Figure 3 shows a regional distribution of the global strain versus time curve. In this figure, the LV was divided into 60 elements from the apex (denoted by A) to the base (B) and from septal to posterior. The regional strain within each element was estimated to be the average of the nodal values of the specific element and the corresponding strain-time curve is shown in a small window. The results show an increasing tendency of the regional strain as the myocardial tissue deforms largely. The regional strain over time representation provides a useful means of localizing abnormalities of cardiac motion and such information is very important for further more detailed clinical investigations.

5. CONCLUSION

We have presented a complete method of myocardial motion analysis from tagged MR images using vector spline techniques. The method combines dynamic tracking of tag deformation, simulating cardiac movement and accurately computing the regional strain distribution. The underlying framework is based on the new development of a class of generalized spline models. Therefore, the applications of the method is not limited to MR data and cardiac motion reconstruction, but might be applied to solve many other types of motion reconstruction problems.

A user-friendly tracking algorithm has been developed to accurately estimate the deformation of tag points during cardiac diastole. The algorithm is capable of tracking in-plane motions from short axis slices and through-plane motions from long axis slices of the heart. The directional information can be incorporated to the vector spline models to produce a three-dimensional representation of the displacement field of myocardial motion. In order to determine material deformation during heart motion, a two-way reconstruction procedure has been performed to the sample directional projections to obtain a vector spline function that establishes a spatial relationship between material points and spatial points. Based on this spline reconstruction, the further quantification of myocardial strain, either linear or nonlinear, becomes trivial by measuring the directional changes in displacement vector. For this reason, the presented cardiac motion analysis method is superior in terms of modeling complex nonlinear deformation of myocardial tissue and computational effectiveness.

The model has been performed on the tagged MRI time sequence. The strain distribution has shown a time-dependent regional change in different parts of the myocardium. The strain over time representation provides an effective way of monitoring and identifying regional abnormalities of myocardial motion. More experiments will be carried out for further investigation of cardiac functions. Future work in this direction also includes automatically tracking epicardial and endocardial contours and the optimization of model parameters.

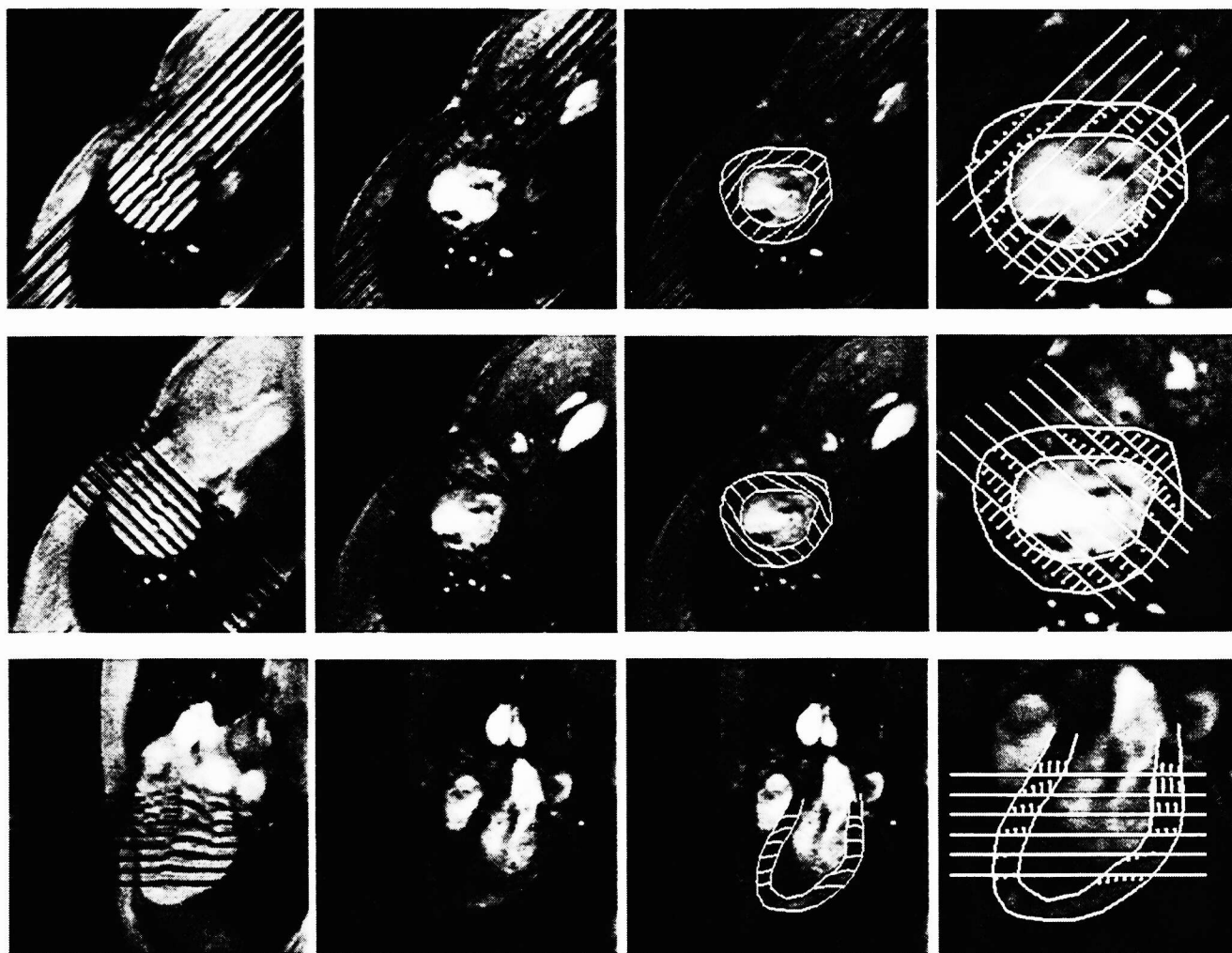


Figure 1. Representative short axis (top two rows) and long axis (bottom row) tagged cardiac images. Images of the first column are the first frames of the time series and correspond to tagging at end systole (due to blood motion, the tag lines are deformed even in the first time frames). The images in the second column were acquired approximately 300ms into diastole. The deformed tags at the final time frames with the outlined epicardial and endocardial surfaces are shown in the third column, and the tag point motion is represented by vectors pointing from the deformed points to their initial positions, shown in the last column. For demonstrating purpose, only a subset of the tag points are shown.

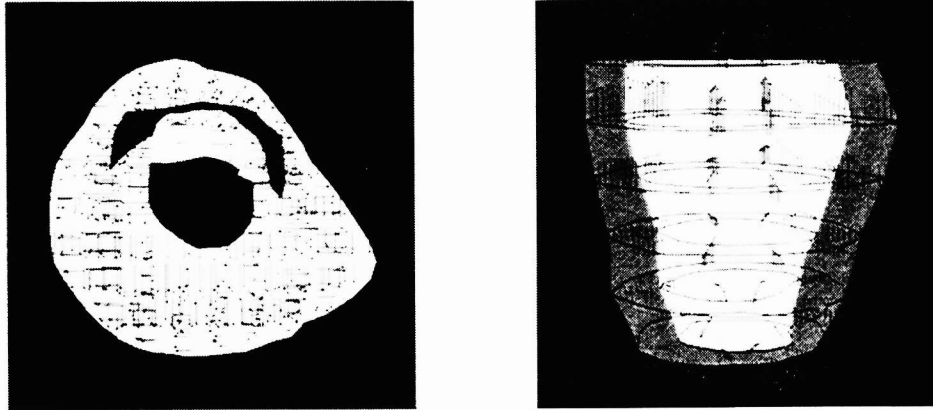


Figure 2. 3D visualization of directional projections. The left figure shows the projection measurements along the X and Y directions, while the projections along Z direction is shown in the right figure. For easy visualization, the X and Y projections are drawn from a short axis view and the Z projections are demonstrated from a long axis view.

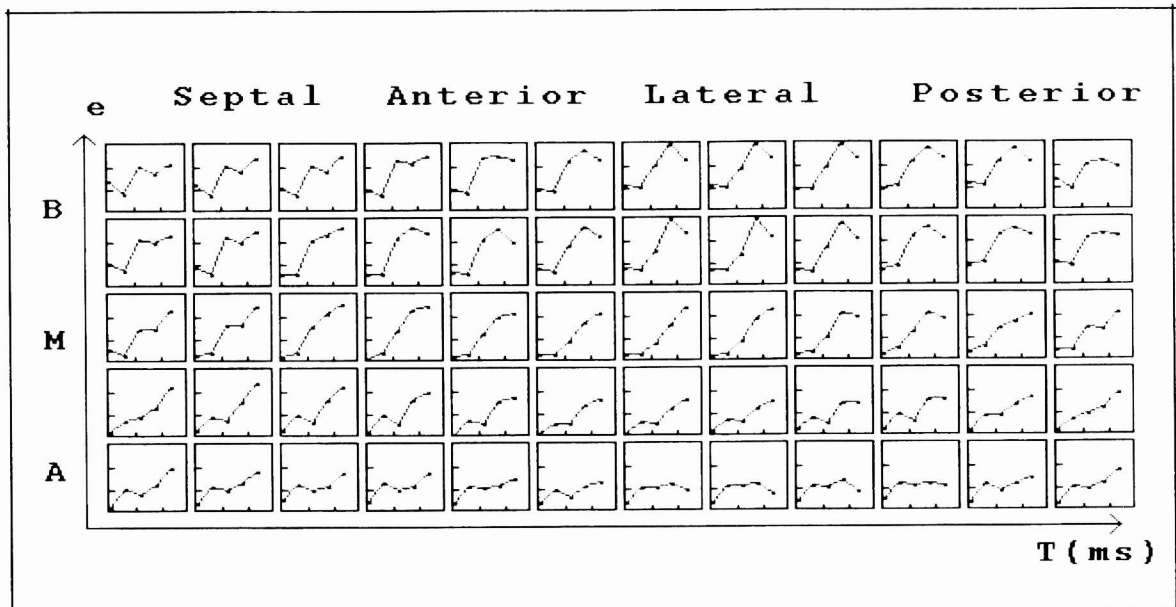


Figure 3. Regional strain maps within myocardium. In this figure, the LV is divided into small elements with eight nodes from apex (A) to base (B), and from septal to posterior. For each element, the average strain vs. time is depicted in a small window, where time changes in the horizontal direction and strain changes in the vertical direction.

ACKNOWLEDGEMENTS

We would like to thank SmithKline Beecham Pharmaceuticals for supporting this work.

REFERENCES

1. F. M. Bengel, M. Schwaiger, "Nuclear medicine studies of the heart," *European Radiology*, **8**(9): 1698-1706, 1998.

2. M. R. Mansoor, G. V. Heller, "Gated SPECT imaging," *Seminar in Nuclear Medicine*, **29**(3):271-278, 1999.
3. E. A. Zerhouni, D. M. Parish, W. J. Rogers, A. Yang, "Shapiro, E. P. Human heart: Tagging with MR imaging – a method for noninvasive assessment of myocardial motion," *Radiology*, **169**:59-63, 1988.
4. L. Axel, L. Dougherty, "Heart wall motion: Improved method of spatial modulation of magnetization for MR imaging," *Radiology*, **172**:349-350, 1989.
5. E. R. McVeigh, E. Atalar, "Cardiac tagging with breath-hold cine MRI," *Magnetic Resonance in Medicine*, **28**:318-327, 1992.
6. S. Kumar, D. Goldgof, "Automatic tracking of spamm grid and the estimation of deformation parameters from cardiac MR images," *IEEE Transaction on Medical Imaging*, **13**(1):122-132, March 1994.
7. A. A. Amini, J. Duncan, "Bending and stretching models for LV wall motion analysis from curves and surfaces," *Image and Vision Computing*, **10**(6):418-430, 1992.
8. A. A. Amini, R. W. Curwen, J. C. Gore, "Snakes and splines for tracking nonrigid heart motion," *Computer Vision – ECCV'96*, II:251-261, Cambridge UK, April 1996.
9. A. A. Young, L. Axel, "Non-rigid heart wall motion using MR tagging," Proc. *CVPR'92 IEEE*, 399-404, 1992.
10. A. A. Young, L. Axel, "Three-dimensional motion and deformation of the heart wall," *Radiology*, **185**:241-247, 1992.
11. D. L. Kraitchman, A. A. Young, C. Chang, L. Axel, "Semi-automatic tracking of myocardial motion in MR tagged images," *IEEE Transactions on Medical Imaging*, **14**(3):422-433, 1995.
12. A. A. Young, D. L. Kraitchman, L. Dougherty, L. Axel, "Tracking and finite element analysis of stripe deformation in magnetic resonance tagging," *IEEE Transactions on Medical Imaging*, **14**(3):413-421, september 1995.
13. L. D. Cohen, I. Cohen, "Finite element methods for active contour models and ballons for 2D and 3D images," *IEEE Transactions on Pattern Analysis and Machine Intelligence*, **15**(11):1131-1147, 1993.
14. T. McInerney, D. Terzopoulos, "A dynamic finite element surface model for segmentation and tracking in multidimensional medical images with application to cardiac 4D image analysis," *Computerized Medical Imaging and Graphics*, **19**(1):69-83, 1995.
15. D. Suter and F. Chen, "Left Ventricular motion reconstruction based on elastic vector splines," Revised version under review by *IEEE Transaction on Medical Imaging*, 1999.
16. M. Kass, A. Witkin, D. Terzopoulos, "Snakes: Active contour models," *International Journal of Computer Vision*, **1**(4):321-331, 1988.
17. L. D. Cohen, "Note on active contour models and ballons," *CVGIP: Image Understanding*, **53**(2):211-218, 1991.
18. M. A. Guttman, J. L. Prince, E. R. McVeigh, "Tag and contour detection in tagged MR images of the left ventricle," *IEEE Transactions on Medical Imaging*, **13**(1):74-88, 1994.
19. W. G. O'Dell, C. C. Moore, W. C. Hunter, E. A. Zerhouni, E. R. McVeigh, "Three-dimensional myocardial deformations: Calculation with displacement field fitting to tagged MR images," *Radiology*, **195**:829-835, 1995.
20. Y. C. Fung, *A first course in continuum mechanics*, Prentice Hall, 1969.